Hindawi
Shock and Vibration
Volume 2024, Article ID 8415703, 15 pages
https://doi.org/10.1155/2024/8415703

Research Article

Research and Application of Coal Seam Permeability Improvement Technology by Sectional Directional Hydraulic Fracturing

Feng Wang [1,2]

[1]*CCTEG Shenyang Research Institute, Shenyang, Liaoning 110016, China*
[2]*State Key Laboratory of Coal Mine Safety Technology, Fushun, Liaoning 113122, China*

Correspondence should be addressed to Feng Wang; fengjob124@163.com

Received 2 November 2023; Revised 15 January 2024; Accepted 27 January 2024; Published 29 February 2024

Academic Editor: Cecilia Surace

To address the challenging issue of gas control in the working faces of the Hegang mining area, based on segmented directional hydraulic fracturing technology, ABAQUS simulation software was employed to simulate and analyze the fracturing process of coal-rock masses under the action of segmented hydraulic fracturing. The study focused on the engineering application research within the mining roadway of the 23# coal seam in the Junde Coal Mine, China. The results indicate that the numerical simulation analysis reveals elliptical patterns in the stress, strain, and fracture width variation of the coal-rock masses influenced by the fracturing action. The width of the fractures exhibits a periodic variation pattern, initially increasing and then slightly decreasing with the injection of water pressure. Additionally, each successive variation shows a decreasing magnitude. After applying segmented hydraulic fracturing technology, the average gas extraction concentration increased by a maximum of 1.73 times, the average mixed flow rate increased by a maximum of 2.16 times, and the average gas extraction pure quantity increased by a maximum of 3.10 times. Segmented hydraulic fracturing can effectively improve gas extraction efficiency, reduce coal seam gas content, and have a depressurizing effect on coal-rock layers. The research findings provide new means for safe and efficient coal mining, particularly in enhancing gas extraction efficiency, alleviating strata pressure, and preventing gas disasters.

1. Introduction

The shallow coal resources in China are rapidly running out due to ongoing growth and use, and deep coal mining is now being carried out more often. However, the gas component of deep coal seams rises as coal mining depths grow. It is simple to cause coal and gas outburst catastrophes under the coal occurrence circumstances of high ground stress, high ground temperature, and high osmotic pressure, which poses a severe danger to the mine's safe operation. One of the key strategies for avoiding coal mine gas mishaps is coal seam gas predrainage. Gas predrainage may be accomplished by positioning bedding boreholes in coal seams to predrainage coal seam gas. Deep coal seams' limited permeability, however, results in inefficient gas extraction. Therefore, carrying out coal seam permeability enhancement treatment to increase coal seam permeability is crucial for the prevention and management of gas catastrophes.

When drilling through coal seams for predrainage, the borehole protrudes, injecting dynamic energy into the coal, creating voids, and relieving the in situ stress. Scholars first highlighted the enhancing effect of borehole protrusion cavitation on coal permeability and designed a protrusion control system to ensure the flow and separation of protruded material in a relatively closed environment [1]. Permeability is a crucial parameter characterizing reservoir fluid flow and production. Scholars conducted experimental research on supercritical CO^2 seepage, permeation, and adsorption in coal seams, considering the influence of injection pressure and temperature. They compared the changes in longitudinal wave velocity before and after the experiment, determining the permeation impact of

supercritical CO^2 on the original coal specimens [2]. Some researchers proposed microwave heating to enhance coal permeability, employing an electromagnetic-thermal-mechanical coupling model for simulation and demonstrating the effectiveness of microwaves in increasing coal permeability [3]. Scholars investigated fluid injection-induced hydraulic fracturing and shear fracturing through laboratory experiments. The results indicated that the closure of hydraulic extension fractures significantly inhibited the permeability enhancement effect of hydraulic fracturing treatment [4]. Researchers suggested a combined method of hydraulic slotting and hydraulic fracturing to improve the permeability of low-permeability coal seams in China. By analyzing the microstructure development and strength characteristics of coal, they established a damage criterion for water-containing gas coal, accurately describing the damage mechanism of gas-containing coal under hydraulic measures and revealing the damage mechanism of coal under oscillating water jet action. This provided a new approach to studying the damage mechanism of pores and cracks under high-pressure jetting [5]. Scholars proposed the basic assumptions of the coal-gas-solid coupling model and introduced the permeability enhancement coefficient of the equivalent interlayer distance for the first time. They developed a mathematical model for the evolution of permeability in protected coal seams during underlying protective layer mining. Using the proposed mathematical model for numerical simulation, they determined the dynamic evolution patterns of stress and permeability in the protected layer as the protective layer face advanced [6].

The purpose of hydraulic fracturing is to increase the gas permeability of coal seams by injecting high-pressure fracturing fluid into fractures. Due to the presence of natural fractures, it is challenging to accurately identify and predict the initiation and propagation of hydraulic fractures. Scholars, based on a two-dimensional particle flow code (PFC2D), established five typical coal models to simulate hydraulic fracturing in coal seams. The research results indicate that the presence of natural fractures has a significant inducing effect on the initiation and propagation of hydraulic fractures, contributing significantly to the increase in the number of fractures and the growth rate of porosity [7]. Researchers found that the minimum horizontal stress difference is a crucial geological factor controlling the vertical extension of mixed fractures. There is a critical displacement of fracturing fluid during the combined fracturing process. Mixed fractures will break through the formation interface and penetrate into adjacent layers when reaching critical displacement. High viscosity fracturing fluid is favorable for the vertical expansion of hydraulic fractures [8]. The geometric shape of hydraulic fractures in the vertical plane is complex, unlike simple fractures in homogeneous reservoirs. To clarify this, a finite element method with a viscous band, including macroscopic lithology contributions, was used to simulate and analyze hydraulic fracturing expansion. It was found that interbedded higher elastic modulus imposes a limiting effect on the height of hydraulic fractures [9]. Scholars, through underground dissection and surface joint measurements, established a visible natural fracture spatial system and concluded that the expansion of hydraulic fractures is controlled by the orientation of natural fractures and the principal stress [10]. The scholars presented experiments involving hydraulic fracturing and gas permeation using raw coal under different stress conditions. They established a permeability model for coal subjected to hydraulic fracturing with an increased stimulated reservoir volume (SRV). The permeability of coal treated with SRV was found to be approximately two to three orders of magnitude higher than before fracturing [11]. In order to understand the gas permeation characteristics and enhance permeability mechanisms of coal under unloading stress conditions, scholars conducted temperature shock, permeability tests, NMR, CT, and SEM scanning experiments on coal samples. After temperature shock, the anisotropy and excessive thermal stress of coal are fundamental causes for coal damage and changes in permeability. An improved nonlinear permeability model for non-Darcy gas flow within fractured coal was established, effectively capturing the nonlinear variations in gas permeability. This model outperforms the traditional Darcy model in describing the nonlinear gas flow in gassy coal [12, 13]. Scholars, building upon conventional energy calculation equations, introduced pore pressure through an effective stress equation and innovatively refined various energy components for gassy coal [14].

In summary, high-pressure hydraulic fracturing technology is employed to alter the physical properties of reservoir rocks, increasing porosity and permeability, and facilitating easier gas extraction through fractured fissures. Traditional extraction involves drilling through coal seams using layer-by-layer drilling, directional long-hole drilling, among other methods. In contrast, segmented hydraulic fracturing technology aims solely to increase porosity and permeability, enhancing extraction efficiency. Current research predominantly focuses on modifying hydraulic fracturing equipment to improve fracturing effectiveness and understanding the impact of different fracturing parameters. However, there is limited research on the fracture propagation patterns of segmented hydraulic fracturing technology and the evolution characteristics of coal stress and strain. This paper takes the Junde Coal Mine in the Hegang mining area, where combined dynamic disasters of ground pressure and coal and gas outbursts are severe, as an example. Building on previous studies, the feasibility of implementing segmented hydraulic fracturing technology in the Junde Coal Mine is explored. Utilizing ABAQUS numerical simulation software and embedding cohesive elements, a finite element model is established to analyze the evolution characteristics of coal stress, strain, and fracture width under the influence of segmented hydraulic fracturing. The study aims to validate the feasibility of enhancing coal seam permeability through segmented hydraulic fracturing technology, providing valuable references for on-site construction of segmented hydraulic fracturing.

2. Staged Hydraulic Fracturing Technology

2.1. Composition of Staged Hydraulic Fracturing Device. Segmented directional hydraulic fracturing antireflection technology and equipment address the limitations of traditional coal seam hydraulic fracturing, characterized by single borehole fracturing with uncontrollable crack propagation direction, poor antireflection effects, bulky fracturing equipment, and high economic costs. Illustrated in Figure 1, the staged hydraulic fracturing device comprises a high-pressure pump station system and a staged fracturing device. The staged fracturing device includes a high-pressure expansion capsule and a decompression fracturing device, while the high-pressure pump station system encompasses a high-pressure pump station, a liquid tank, and a program control system. During the hydraulic fracturing of the coal seam, water from the liquid tank is injected into the expansion capsule through the pipeline via the high-pressure pump. The pressure of the water entering the capsule can be adjusted using the relief valve's knob. As the capsule expands and pressure builds up, the water injector valve opens, allowing high-pressure water to enter the coal seam, inducing fracture in the coal seam. This technology and equipment combination effectively overcomes the drawbacks of traditional methods, ensuring controlled and directed fracturing with improved antireflection effects, reduced equipment volume, and lower economic costs [15–21].

2.2. Principle of Staged Hydraulic Fracturing. Oilfield stimulation techniques were the first to employ hydraulic fracturing technology. Since 1970, China has created and used this technology in coal mines to improve gas extraction efficiency and raise the permeability coefficient of coal seams [22–24]. The coal seam's initial permeability was often low since it is typically buried well below, supporting the weight of the strata above it, and its fissures are compressed and in a closed or semiclosed state. The evolution of a coal seam crack caused by hydraulic fracturing is shown in Figure 2. Drilling is used in hydraulic fracturing to pump a lot of liquid into the coal seam. When the liquid pressing speed exceeds the coal seam's inherent ability to absorb water, the liquid pressure will progressively grow owing to an increase in flow resistance. The initially closed crack inside the coal seam will open when the pressure of the rock layer above the coal seam is surpassed. In addition, when the pressure of the injected liquid rises to exceed the coal wall's tensile strength, stress concentration forms at the crack's tip, causing the fracture to grow into the next weak surface and produce further artificial cracks. The initial coal seam cracks that form as a result of the coal seam's opening and growth widen and connect to form a fracture network, which changes the coal seam's gas flow state from diffusion to nonlinear seepage to linear seepage and improves the coal's permeability. The desorption impact of coal adsorption gas may also be increased by an increase in cracks, allowing more adsorbed gas to be transformed into free gas and accelerating extraction while decreasing the gas amount in the coal seam and enhancing gas extraction efficiency [25–29].

The whole borehole is often subjected to standard hydraulic fracturing, as shown in Figure 3(a). A cylindrical surface makes up the first area of hydraulic action, and its length can range from tens to hundreds of meters. The hydraulic fracturing technique involves a lot of water seepage, which necessitates a lot of water flow to maintain enough water pressure. After the borehole fractures, the fracturing generally continues in a weaker location as long as the crack expands on a weak surface and stops developing in other directions. Therefore, with the length increase of the borehole fracturing section, the amount of large cracks does not always show an increasing trend.

The staged hydraulic fracturing technique outperforms the conventional hydraulic fracturing technology, as illustrated in Figure 3(b). By utilizing a unique packer, the entire borehole is divided into many parts, and the pressure is concentrated at a single point each time for fracturing. In other words, the action surface of conventional hydraulic fracturing is converted to the action point, and then, the procedures are carried out in a certain order. Due to the comparatively concentrated action point, the seepage water pressure is decreased, the effective water pressure is enhanced, and the smaller flow rate may acquire a good fracturing effect and lower the water flow, therefore minimizing the need for the fracturing hydraulic system. The equipment's capacity has been drastically decreased so that it can better fit the subterranean roadway requirements.

The high-pressure water injection pump, hole sealing device, water injector, high-pressure water injection pipe, and other components make up the bulk of the staged hydraulic fracturing equipment [30–33]. The exit is situated in between the two capsules that seal the sealing mechanism. There is no open surface around the coal when single-hole hydraulic fracturing is performed on a coal seam, thus cracks can only form when additional coal components are compressed or the surrounding rock is supported. The pressure relief ring that forms around the control hole after it is constructed is used to guide the crack to expand in the direction of the control hole and ultimately communicate with the control hole in the implementation of point fracturing if a parallel borehole is built as a control hole at a specific distance around the fracturing borehole [28, 34]. In order to produce directional fracture, as illustrated in Figure 4(a), high-pressure water even removes certain coal chunks from the ground. This reduces ground stress and increases permeability. The control hole can also be utilized as a drainage hole once the fracturing is done. Because the damage zone formed between the fracturing hole and the control hole can be used as a channel for gas seepage, the gas far from the borehole is extracted from the borehole, thereby increasing the coal seam's permeability, increasing the drainage effective area, and improving the extraction rate, as shown in Figure 4(b).

2.3. Ground Segmented Hydraulic Fracturing Test. The purpose of the ground staged hydraulic fracturing test is to process different types of capsules so that they can be applied

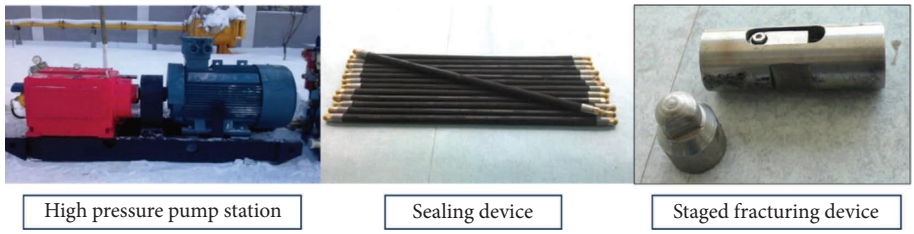

Figure 1: Sectional hydraulic fracturing device.

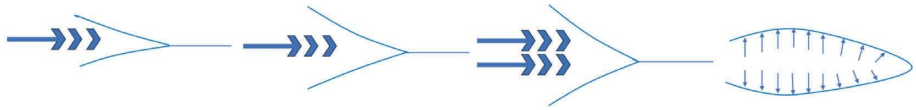

Figure 2: Crack development process under hydraulic fracturing.

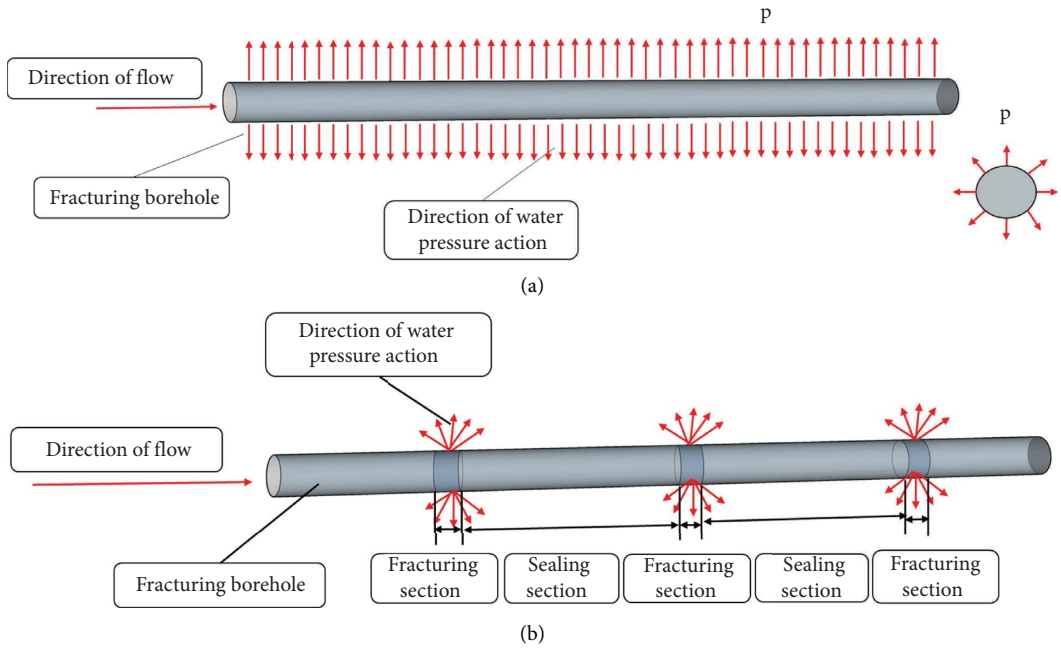

Figure 3: Hydraulic fracturing mode of action. (a) Traditional "face" hydraulic fracturing. (b) Segmented "point" hydraulic fracturing.

to boreholes of different diameters. The schematic diagram of the experimental system is shown in Figure 5.

Utilizing the overflow valve, the high-pressure pump introduces water from the liquid tank into the expansion capsule. The pressure of the water entering the capsule is controlled by adjusting the knob on the overflow valve. Subsequently, due to the expansion and increasing pressure of the capsule, high-pressure water flows into the steel pipe through the water injector valve's opening. The water pressure within the sealing portion, containing the water injector, can be monitored using a pressure gauge. Additionally, a stop valve is employed to facilitate pressure relief. Each piece of laboratory equipment is visually presented in Figure 6.

Analysis indicates that the expansion and sealing effects of the capsule are directly influenced by the elastic coefficient of the spring in the water injector. There are two situations in which the spring elastic coefficient is inappropriate:

(1) The water injector's spring is compressed, the water injection port is opened, the pipe pressure is raised, and the capsule is forced out of the steel pipe when the spring elastic coefficient is too low and the high-pressure water has not had time to expand the capsule

(2) When the spring elastic coefficient is low, the high-pressure water expands the capsule, but when the water injector's water injection port is opened, the

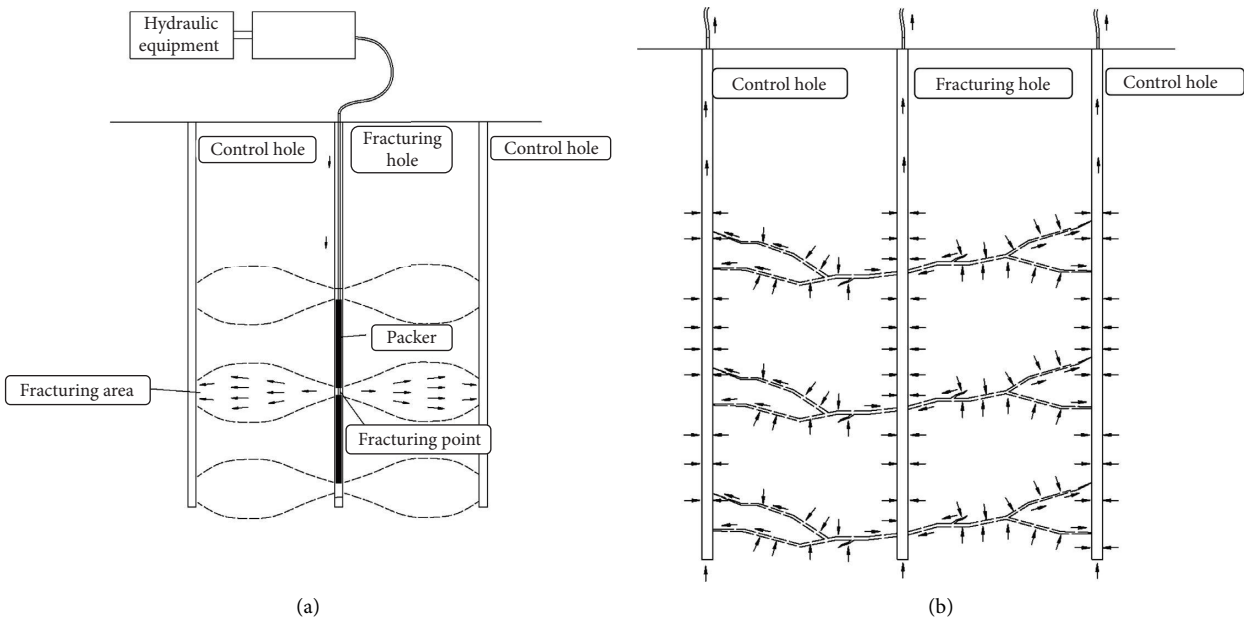

Figure 4: Borehole arrangement of segmented point directional fracturing test. (a) Sectional directional hydraulic fracturing arrangement. (b) Sectional directional hydraulic fracturing fracture propagation.

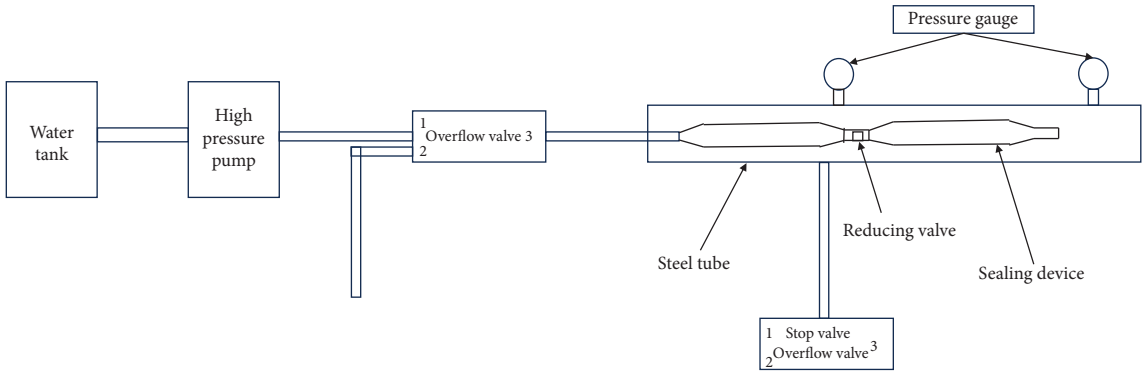

Figure 5: Experimental principle of staged hydraulic fracturing.

pressure inside the capsule is insufficient, and there is not enough friction between the steel pipe and the capsule to withstand the sealing section's pressure, which will also force the capsule out of the steel pipe

As depicted in Figure 7, several springs with varying elastic coefficients were selected for testing. Ultimately, it was determined that the specifications of the No. 3 spring best matched the requirements of the capsule.

After completing the experimental equipment connection, the overflow valve knob is opened. Once each interface is verified to have a secure connection, the power supply for the high-pressure pump is activated. Initially, high-pressure water does not reach the capsule but instead flows out of the overflow valve outlet. The relief valve knob is then adjusted slowly. As the capsule begins to expand and the pressure gauge data on the relief valve rises, the water injector valve remains closed, and the pressure gauge on the steel pipe does not register any reading. Continuing to adjust the overflow valve knob to increase the pressure inside the capsule, the water injector valve opens when the pressure surpasses its operating threshold. This is evidenced by a rise in pressure gauge data. Currently, the pressure gauge value is approximately 4 MPa lower than the overflow valve's pressure gauge, indicating that the opening and closing pressure values of the water injector valve are approximately 4 MPa. With continuous injection of high-pressure water, the pressure gauge value will keep rising. To mitigate the risk of excessive pressure, the stop valve's knob can be turned to regulate the sealing section's pressure at this moment. Furthermore, following the test, the stop valve functions as a pressure release valve.

3. Numerical Simulation Analysis

3.1. Model Establishment. Using ABAQUS numerical simulation software, a three-dimensional model measuring 40 m by 100 m by 43 m was constructed. The model's

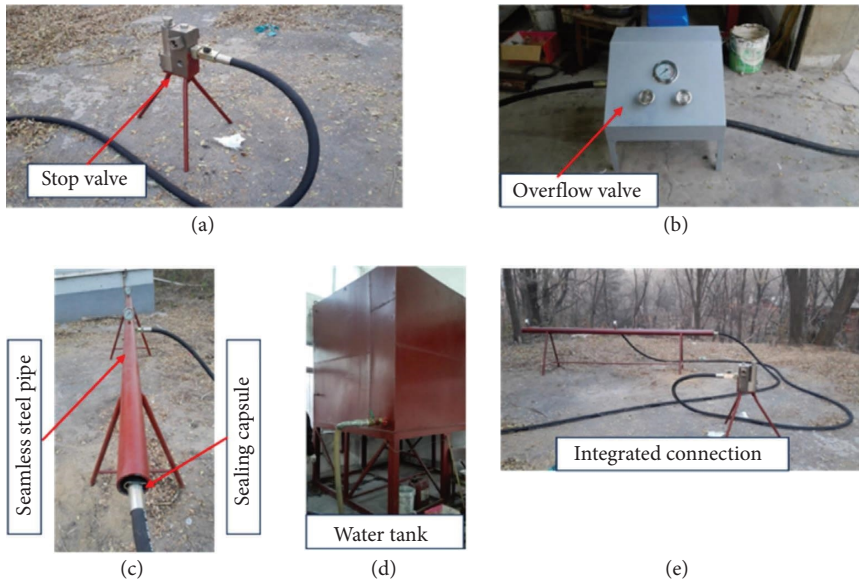

Figure 6: Sectional hydraulic fracturing test.

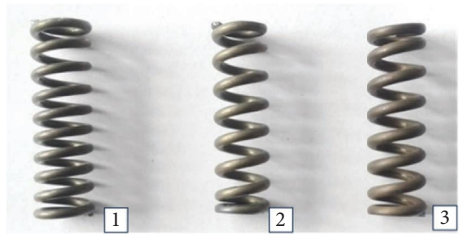

Figure 7: Springs with different elastic coefficients.

surrounding boundary conditions were constrained through displacement. To divide the model into left and right halves, a layer of zero thickness cohesive unit layer was introduced. This cohesive unit layer effectively emulates the properties of medium deformation and fracture propagation under pressure. The center position of the cohesive unit layer was selected as the water pressure injection point for staged hydraulic fracturing, aiming to accurately replicate the fracture propagation characteristics of coal and rock mass during staged hydraulic fracturing. To simulate the expansion of the damaged and destroyed portion of the model due to compression cracks along the first damage element from the water pressure injection site, four initial damage elements were created around the water pressure injection point. Figure 8 illustrates the grid division of the model, which consists of 104625 nodes and 96480 units. The model is mainly divided into three layers, in which the middle section of the coal seam is the main fracturing area, and the thickness of the coal seam is 3 m. In the model, the roof and floor of the coal seam are divided into interlayers, and the thickness of the interlayer is 20 m. The unit type of the model is C3D8P, and the unit type of the cohesive unit layer is C3D8P (considering seepage). The relevant parameters in the model are shown in Table 1.

3.2. Analysis of Crack Propagation Direction. In the process of staged hydraulic fracturing of a coal seam, the distribution characteristics of reservoir and roof and floor stress play a pivotal role in controlling the effectiveness of staged hydraulic fracturing. During the staged hydraulic fracturing of coal seams, the development of fractures typically aligns with the direction of the minimum horizontal principal stress, occasionally following the orientation of primary fractures or bedding extension locally. However, in general, the fractures tend to extend along the direction of the maximum horizontal principal stress. Combining findings from relevant research, it is deduced that there exists a certain correlation between the rock characteristics of the reservoir and the direction of horizontal in situ stress, as expressed in equation (1), where σ_h and σ_H represent the minimum and maximum horizontal principal stresses, respectively.

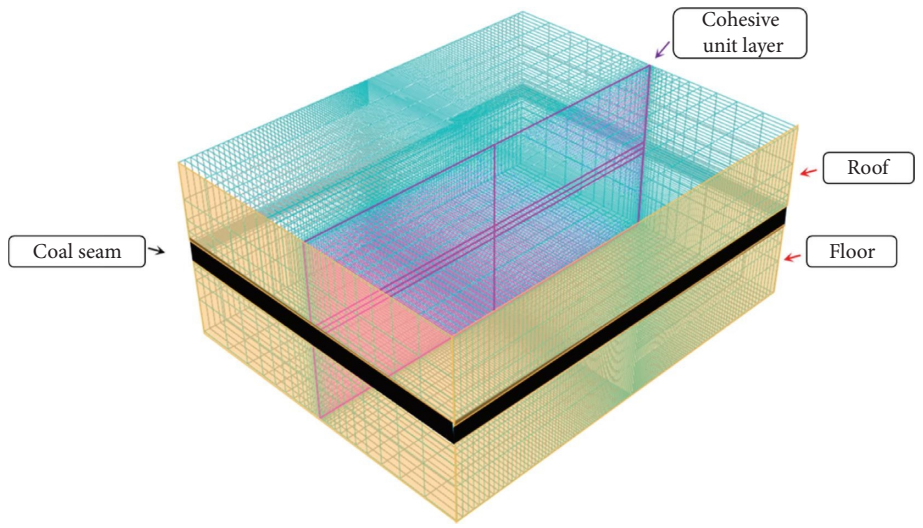

Figure 8: Three-dimensional numerical simulation grid division.

Table 1: Related parameters of staged hydraulic fracturing model.

Object	Parameter	Numerical value
Reservoir	Elastic modulus/GPa	3.5
	Poisson's ratio	0.2
	Permeability	1×10^{-7}
	Porosity ratio	0.2
	Crustal stress (σ_h, σ_H, σ_V)/MPa	5, 9, 10
Interlayer	Elastic modulus/GPa	20 GPa
	Poisson's ratio	0.25
	Permeability	1×10^{-9}
	Porosity ratio	0.2
	Crustal stress (σ_h, σ_H, σ_V)/MPa	5, 10, 10
Fluid properties	Fluid leak off/(m/s)	1×10^{-4}
	Fracturing fluid viscosity/(Pa/s)	1×10^{-3}
	Fracturing fluid density/(kg/m^3)	9800
	Input pickup rate/(m^3/s)	1×10^{-4}

$$\begin{cases} \sigma_h = \dfrac{v}{1-v}\left(\sigma_V - \alpha P_p\right) + \dfrac{E\varepsilon_H}{1-v^2} + \dfrac{vE\varepsilon_h}{1-v^2} + \alpha P_p, \\ \sigma_H = \dfrac{v}{1-v}\left(\sigma_V - \alpha P_p\right) + \dfrac{E\varepsilon_h}{1-v^2} + \dfrac{vE\varepsilon_H}{1-v^2} + \alpha P_p, \end{cases} \tag{1}$$

where E is the elastic modulus of rock, GPa; v is the Poisson's ratio of rock, dimensionless; α is Biot's porous elastic coefficient, dimensionless; P_p is rock pore fluid pressure, MPa; ε_H is the strain in the direction of the maximum horizontal principal stress, %; and ε_h is the strain in the direction of the minimum horizontal principal stress, %.

Analyzing the equation above reveals that the maximum and minimum principal stresses are primarily influenced by the mechanical parameters of the rock layer, Biot's porous elastic coefficient, and pore fluid pressure. Notably, the Biot porous elastic coefficient and pore fluid pressure are independent of the reservoir lithology. The variation in rock mechanics parameters significantly affects the magnitude of in situ stress within the reservoir. Consequently, horizontal stress is predominantly governed by the rock mechanics parameters, specifically the elastic modulus and Poisson's ratio of the rock layer.

In the context of staged hydraulic fracturing of the coal seam, the roof and floor exhibit higher strength than the coal seam, resulting in a larger minimum horizontal principal stress (σ_h). This condition is more likely to impede the extension of the crack tip. On the contrary, the coal seam, characterized by lower strength and higher damage, has a relatively smaller minimum horizontal principal stress (σ_h). When the crack tip encounters the coal seam, it is more prone to develop and extend into the reservoir.

3.3. Crack Propagation Criterion. The traction separation criteria are followed by the fracture propagation characteristics of the cohesive unit layer during simulated fracturing [35–39]. Figure 9 depicts the schematic representation of the traction separation criterion. Pressure progressively displaces the cohesive unit, and the traction force inside the unit is inversely proportional to the displacement. The unit stiffness k is the slope of the traction force and displacement. The traction force grows together

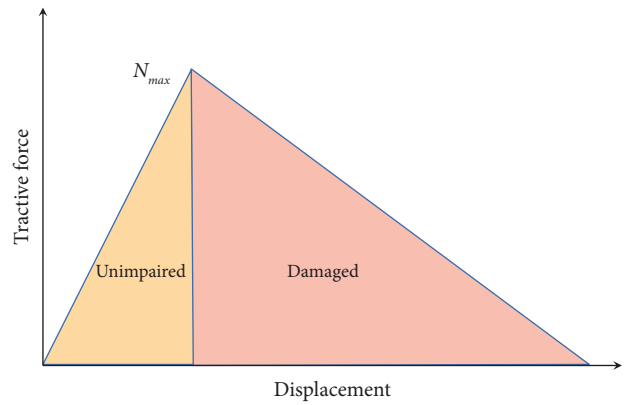

Figure 9: Schematic diagram of traction separation criterion.

with the displacement. When the traction force exceeds the unit's failure strength $N_{\max}$, it will start to decline as the displacement rises, indicating that the material is being destroyed and that its cohesive force is continuing to decline. Equations (2) and (3) are the calculation equations for the failure strength of the cohesive unit. When the model is embedded in the cohesive unit layer, the thickness in the model is zero, but an effective thickness needs to be defined in the actual calculation. The effective thickness defined in this model is 0.001 m.

$$\mathbf{k} = \frac{\mathbf{E}}{\mathbf{h_{eff}}}, \tag{2}$$

$$\mathbf{T} = \begin{cases} \mathbf{k}\delta, & \delta \le \delta_{\mathbf{0}}, \\ (\mathbf{1} - \mathbf{D})\mathbf{k}\delta, & \delta_{\mathbf{0}} < \delta \le \delta_f, \\ \mathbf{0}, & \delta > \delta_f, \end{cases} \tag{3}$$

where k is the cohesive element's stiffness, MPa/m; e is the material's elastic modulus, MPa; h_{eff} is the set cohesive effective thickness, m; δ, δ_0, and δ_f are the relative displacements caused by the unit's hydraulic fracturing, the initial deformation, and total destruction, respectively, m; D is the damage factor. When $D = 0$, the material is considered to be harmed, whereas when $D = 1$, the substance has been totally destroyed.

When simulating the fluid flow in staged hydraulic fracturing, the fluid in the simulation is incompressible, and the direction of fluid flow only flows along the cohesive unit. The direction of fluid flow can be divided into two types. One is tangential flow, which dominates the expansion of fractures affected by staged hydraulic fracturing. The other is normal flow. The fluid flows along the normal direction and dominates the fluid loss in the fracture. Most of the fluid flows along the tangential direction of the unit under the pressure of the water pressure injection point, while only a few fluid flows in the normal direction into the lower rock layer. Equations (4) and (5) are the equations for the tangential and normal flow of the fluid along the cohesive unit.

$$\mathbf{q} = -\frac{\omega^3}{\mathbf{12}\mu}\nabla\mathbf{p}, \tag{4}$$

$$\begin{cases} \mathbf{q_t} = \mathbf{c_t}(\mathbf{p_f} - \mathbf{p_t}), \\ \mathbf{q_b} = \mathbf{c_b}(\mathbf{p_f} - \mathbf{p_b}), \end{cases} \tag{5}$$

where q is the flow density vector of the fluid flowing along the tangential direction; ω is the crack propagation displacement, m; μ is the fluid viscosity, Pa·s; ∂_p is the pressure gradient of fluid flow, Pa/m; q_t and q_b are the volume velocity of fluid flowing into the upper and lower strata along the normal direction, m^3/s; c_b and c_t are the unit filtration coefficients of seepage into the upper and lower strata, $m/s^{0.5}$; and p_f, p_t, and p_b are the fluid pressure on the upper, middle, and lower surfaces of the unit, Pa, respectively.

3.4. Analysis of Simulation Results. The graphic output of this staged hydraulic fracturing simulation only displays the stress, strain, and crack propagation width change of the cohesive unit layer because the water pressure injection point, crack initiation point, and crack propagation development are all inside the model. The stress, strain, and fracture propagation width of the coal and rock mass as simulated by staged hydraulic fracturing are shown in Figure 10.

In Figure 10(a), staged hydraulic fracturing induces a significant tensile stress at the water pressure injection point in the coal and rock mass. With increasing injection time, the water pressure rises, and the tensile stress propagates along the weak surface of the coal seam, resulting in tensile failure. The adjacent coal seam, as well as the above and lower strata, is predominantly influenced by the tensile stress generated by water pressure. The fracture point in the coal seam experiences the highest tensile stress, reaching approximately 10 MPa. The tensile stress in the damaged region of the coal-rock mass ranges from 6 to 8 MPa. For the cohesive element to replicate hydraulic fracturing, the fracturing tip unit must be damaged. The tensile stress in the undamaged tip unit increases with the duration of water injection. If the tensile tension in the tip unit surpasses the tensile strength of the coal, the unit becomes damaged, and the fracture advances. The subsequent tip unit becomes the focal point of water pressure until the model achieves the desired precision.

Figure 10(b) displays the strain in the coal and rock mass subjected to compression fracture. In hydraulic fracturing, the coal seam is the primary direction of water flow, and most of the strain evolution occurs in the coal seam due to the robust upper and lower layers. The strain evolution cloud diagram exhibits an oval shape, with the center having a prolonged period until compression fractures occur, and the strain there is significantly greater than in the rest of the oval. The maximum strain is 1.99%. To more accurately represent the changing features of the coal seam fracture

width influenced by compression fracture, the deformation scaling coefficient of the fracture expansion width is adjusted to 600.

In Figure 10(c), the isometric view of fracture expansion width illustrates the maximum fracture width, concentrated in the center of the coal seam and gradually declining from the middle to the periphery. The maximum width is approximately 4 mm, with the smallest surfaces being the tip of hydraulic fracturing and the contact surface between the coal and rock mass.

The fracture propagation width curve at the water pressure injection location is depicted in Figure 11. The graph illustrates that during the initial stage of staged hydraulic fracturing, the fracture propagation width experiences a rapid increase. Within seconds, the fracture propagation width at the water pressure injection point can reach up to 2.5 mm. Subsequently, with the continuous injection of pressurized water at the injection location, the fracture propagation width temporarily decreases. This decline occurs because the coal breaks when pressurized water is continuously injected, surpassing the coal's tensile strength at the injection site. Under the influence of tension from the overlaying rock, the crack in the coal gradually closes as water flows to the deep section of the coal. This leads to a reduction in water pressure at the injection site. However, the injection of water pressure at the location persists. The subsequent noncracking unit accumulates enough water pressure to reopen the closed fracture, although at a slower pace than before. Consequently, Figure 11 illustrates a pattern where the crack expansion width initially grows and then decreases. Furthermore, during water pressure injection, the damaged area in the coal continues to expand, and the crack expansion tip gradually moves farther from the water pressure injection point, exerting less and less influence on it.

In conclusion, the segmented hydraulic fracturing technique studied in this paper proves to be more effective in increasing coal seam permeability. Some scholars have simulated the hydraulic fracturing process using ABAQUS, obtaining results on the expansion of hydraulic fractures under various influencing parameters [8, 40]. The study analyzes the impact of geological and hydraulic fracturing parameters on crack propagation, playing a positive role in predicting the effectiveness of hydraulic fracturing. Through the analysis of simulation results, it is observed that during the initial stages of segmented hydraulic fracturing, the rapid increase in crack expansion width at the water pressure injection point reaches up to 2.5 mm within seconds. Subsequently, with the continuous injection of pressurized water, the crack expansion width experiences a brief decrease. However, as water pressure continues to be injected at the injection point, the next noncracked unit accumulates significant water pressure, leading to the reexpansion of previously closed cracks. Therefore, adopting segmented hydraulic fracturing technology results in increased coal fractures, enhanced permeability, and improved extraction efficiency.

4. Field Application and Effect

4.1. Field Introduction. The Junde Coal Mine has coal seams that can be mined, including the 21# coal seam, 22-1# coal seam, 22-2# coal seam, and 23# coal seam. Each coal seam is prone to spontaneous combustion, and they all experience severe dynamic ground pressure. The 22-2# coal seam is a prominent coal seam with an average strike length of 420 meters, an average dip length of 140 meters, and an average thickness of 2.99 meters. The original gas content is 8.7 m^3/t, and the original gas pressure is 0.85 MPa. According to the "Temporary Regulations on Gas Extraction Standards in Coal Mines" and the "Regulations on the Prevention and Control of Coal and Gas Outbursts," mining operations are allowed when the gas content in the coal seam is less than 5 m^3/t, and the gas pressure is less than 0.5 MPa.

To address the risks of ground pressure, outbursts, and fires in each coal seam, it is necessary to comprehensively consider and manage various disaster systems. Through experiments and ensuring the safety of mine production, a set of safe, reliable, economically reasonable, and technically feasible disaster management methods have been developed, including the segmented directional hydraulic fracturing technology to enhance permeability in coal seams.

4.2. Field Application Scheme. According to the requirements of the segmented hydraulic fracturing technology, the application is implemented in the 23# coal recovery roadway of the Junde Coal Mine in the Hegang mining area. Two sets of fracturing tests are conducted with the following specifications for drilling holes. For each set of fracturing tests, three holes are drilled in the coal recovery roadway. The middle hole is the fracturing hole, and the two side holes are control holes. After the fracturing operation in the fracturing hole is completed, the hole is sealed, connected to the mine extraction system, and the gas extraction flow rate and concentration are regularly measured. For the control group, two normal extraction holes are drilled in the coal recovery roadway. After construction, the holes are sealed, connected to the mine extraction system, and the gas extraction flow rate and concentration are regularly measured. The distance between holes is 10 meters, and the hole depth is designed to be 60 meters. A total of 10 holes are constructed for the two sets of fracturing tests. Specific drilling parameters for each set of fracturing tests in the coal recovery roadway are detailed in Table 2.

Figure 12 illustrates the comprehensive connection diagram of the system. Once the system connection is finalized, personnel are restricted from passing, and a notice is positioned 30 meters before and after the fracture point in the roadway. Initiating the high-pressure pump, the pressure change over time is recorded subsequent to the examination of each interface for stiffness assessment. The pump is then deactivated upon detecting a decrease in pressure and a halt in amplitude increase, indicating communication between the fracture hole and the control hole.

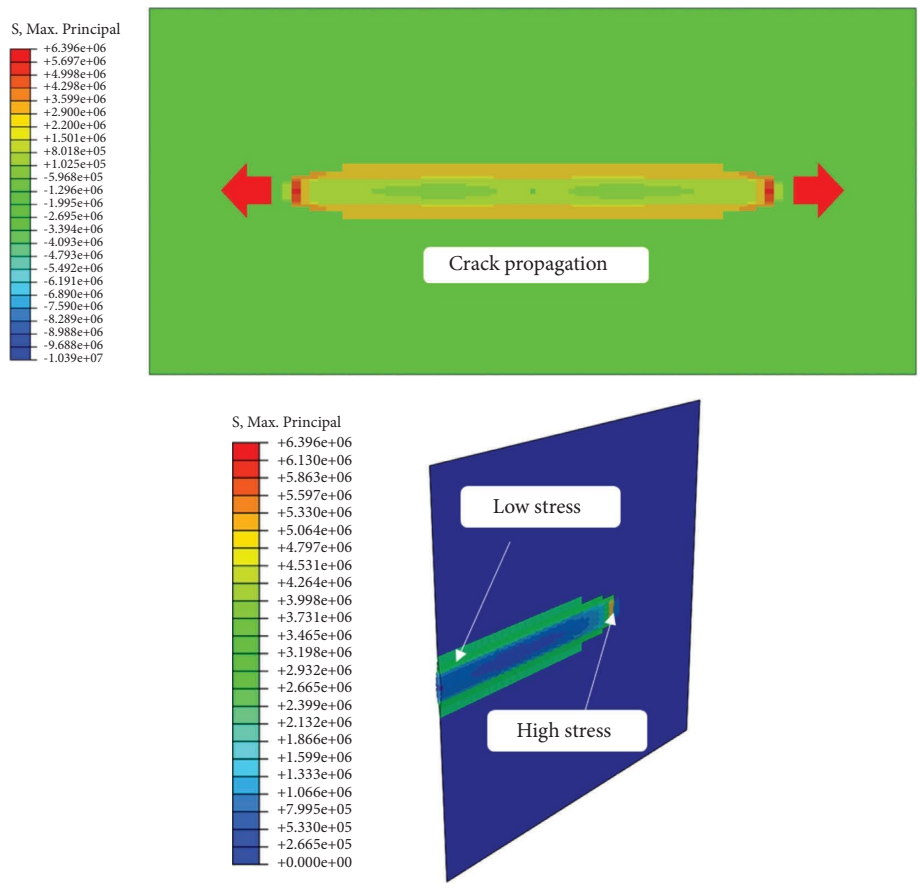

(a)

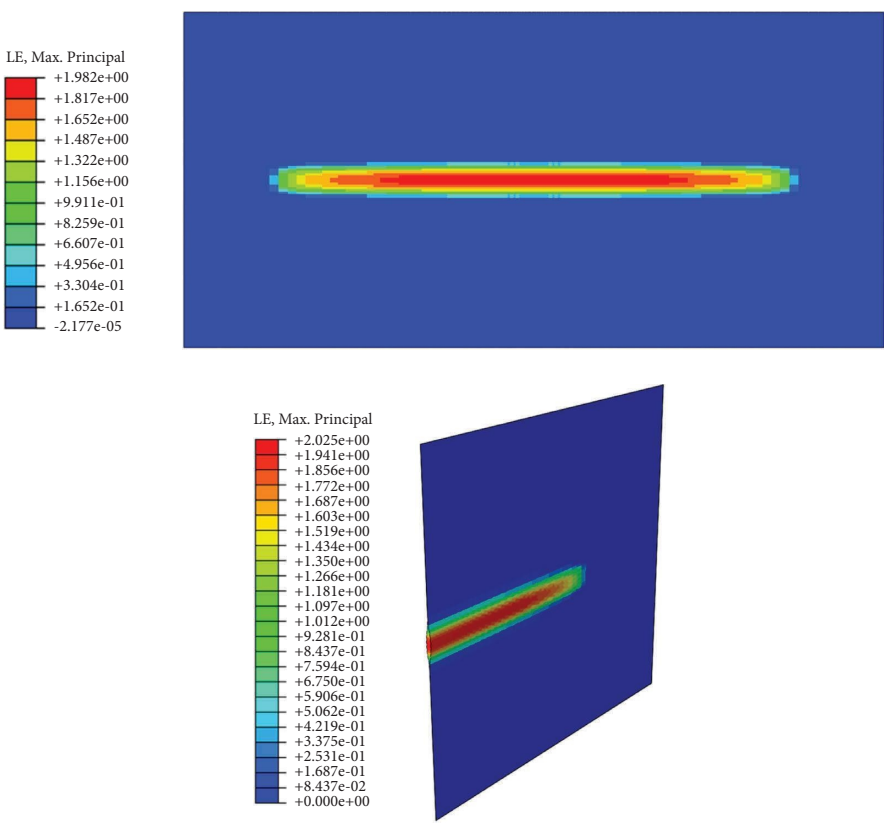

(b)

Figure 10: Continued.

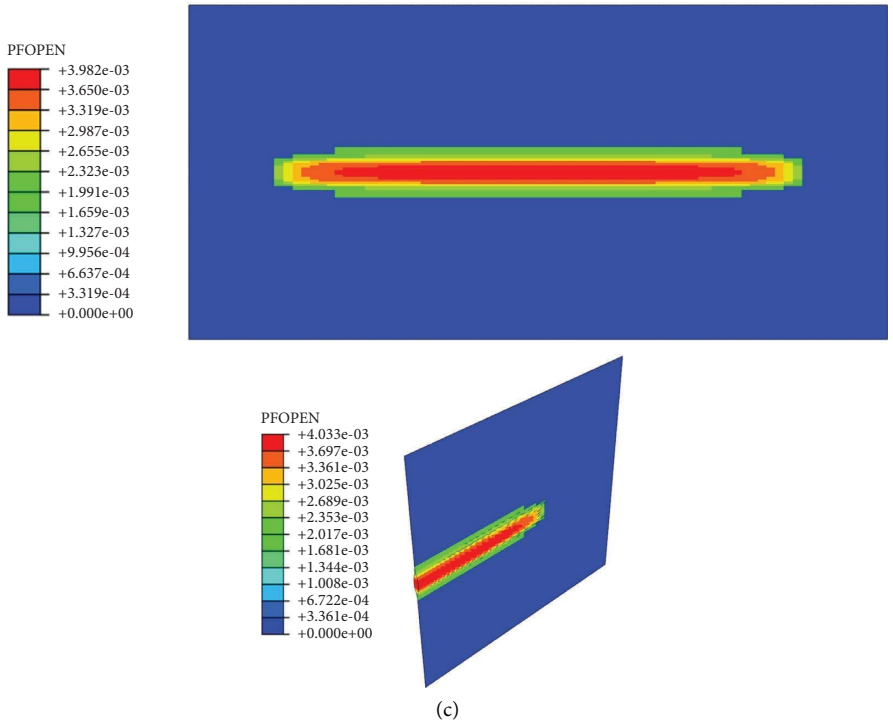

Figure 10: Sectional hydraulic fracturing stress, strain, and crack propagation width. (a) Coal and rock mass fracturing stress changes. (b) Coal and rock strain variation program. (c) Crack propagation width of coal and rock mass.

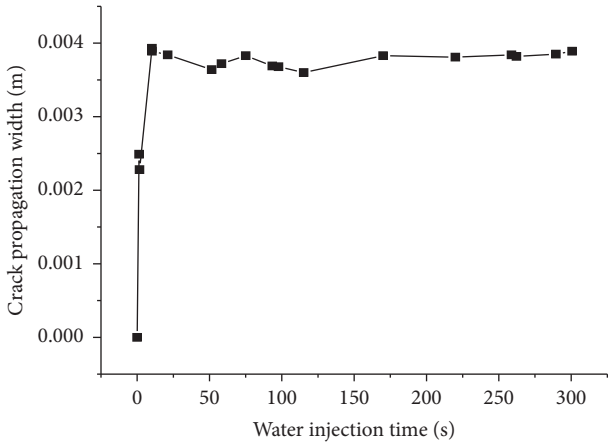

Figure 11: Crack propagation width with water injection time at water injection point.

4.3. Application Effect Analysis. According to the site's real conditions, the No. 1 and No. 2 boreholes in the groove are unfractured. The Nos. 3, 4, and 5 boreholes serve as a comparison group, with No. 4 serving as the fracturing hole and Nos. 3 and 5 serve as control holes. To evaluate the effectiveness of the staged hydraulic fracturing technique, drilling and peeping were done on the nearby rock of fracturing hole No. 4. The peeping holes Nos. 7 and 8 were located 18 meters from the fracturing hole No. 4. On observation holes No. 7 and No. 8, drilling and peeping were carried out after staged hydraulic fracturing. There is no evident fragmentation, and the integrity of the coal seam before hydraulic fracturing is high. After hydraulic fracturing, a lot of fracturing water was seen within Nos. 7 and 8, and the whole borehole was severely damaged, showing that the staged hydraulic fracturing method extends coal seam fissures and has the desired impact of enhancing coal seam permeability.

The primary objective of the fracturing test is to assess the water discharge from the control hole. Fracturing hole No. 4, with a diameter of 94 mm, a depth of 61 m, a 10 m separation from the control hole, and a fracturing period of approximately 65 minutes at a depth of 24 m, was subjected to testing. As depicted in Figure 13, the high-pressure pump initiated the test with an initial pressure of 30 MPa. When the final control hole began filling with water, the water pressure decreased to 20.3 MPa, accompanied by a flow rate of 180 L/min. Approximately 10 tons of water were utilized until the control hole was filled. Once fractured, the borehole was sealed and connected to the gas drainage conduit for gas extraction. Both the control group and the fracture hole were equipped with flow and concentration measurement devices. Daily measurements of mixed flow and gas concentration for each borehole were recorded until the values stabilized, starting about 15 days after the initiation of the drainage system. The numerical time curve is illustrated in Figure 14 based on the actual situation.

The investigation of the extraction impact following segmented hydraulic fracturing reveals significant improvements. The average gas concentration in the observation period has increased by 1.73 times, the average mixed flow has seen a 2.16 times increase, and the average gas extraction has surged by 3.10 times. This indicates that

Table 2: Borehole parameter.

Test site		Drilling number	Drilling diameter (mm)	Drilling depth (m)	Borehole azimuth
23# coal mining roadway	Reference group	1	94	61	Vertical roadway side
		2	94	55	Vertical roadway side
		3	94	62	Vertical roadway side
	Fracturing group	4 (fracturing hole)	94	61	Vertical roadway side
		5	94	61	Vertical roadway side

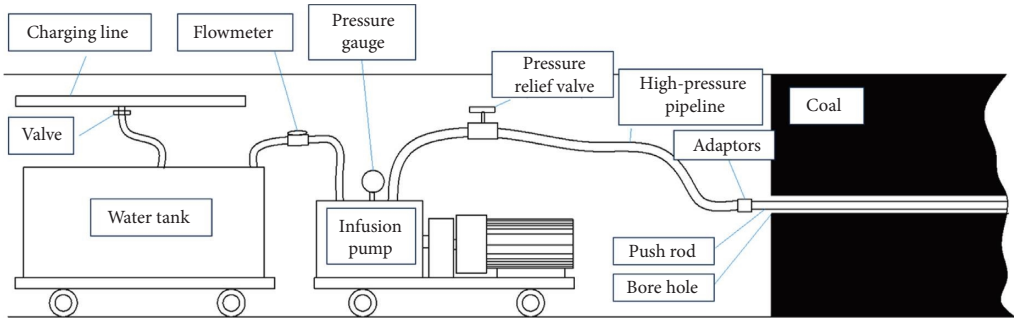

Figure 12: Hydraulic fracturing connection diagram.

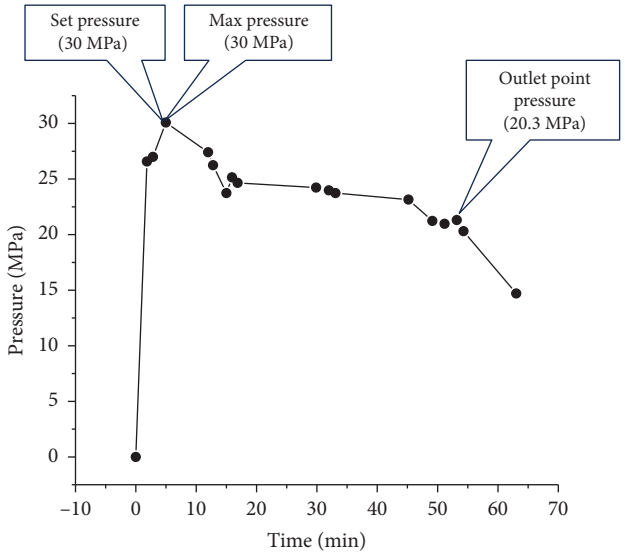

Figure 13: Output pressure of high-pressure pump changing with time.

segmented hydraulic fracturing is effective in reducing the gas content in the coal seam, enhancing gas extraction efficiency, and mitigating the risk of gas-related incidents during mining operations.

One notable advantage is the potential reduction in the number of extraction boreholes required. This is attributed to the considerable increase in coal seam permeability resulting from hydraulic fracturing, leading to an expanded extraction radius for each corresponding borehole. Additionally, hydraulic fracturing contributes to the alleviation of pressure on rock, stress reduction, and a minimized risk of rock breakage. The equipment involved is straightforward, easy to operate, and reusable, presenting promising economic benefits and application possibilities.

5. Discussion

(1) Segmented hydraulic fracturing is a technology used to increase the efficiency of coal seam gas extraction, and its economic feasibility and cost-effectiveness are crucial factors in deciding whether to adopt this technique. The economic analysis of segmented hydraulic fracturing includes initial investment, operating costs, and long-term benefits. Initial

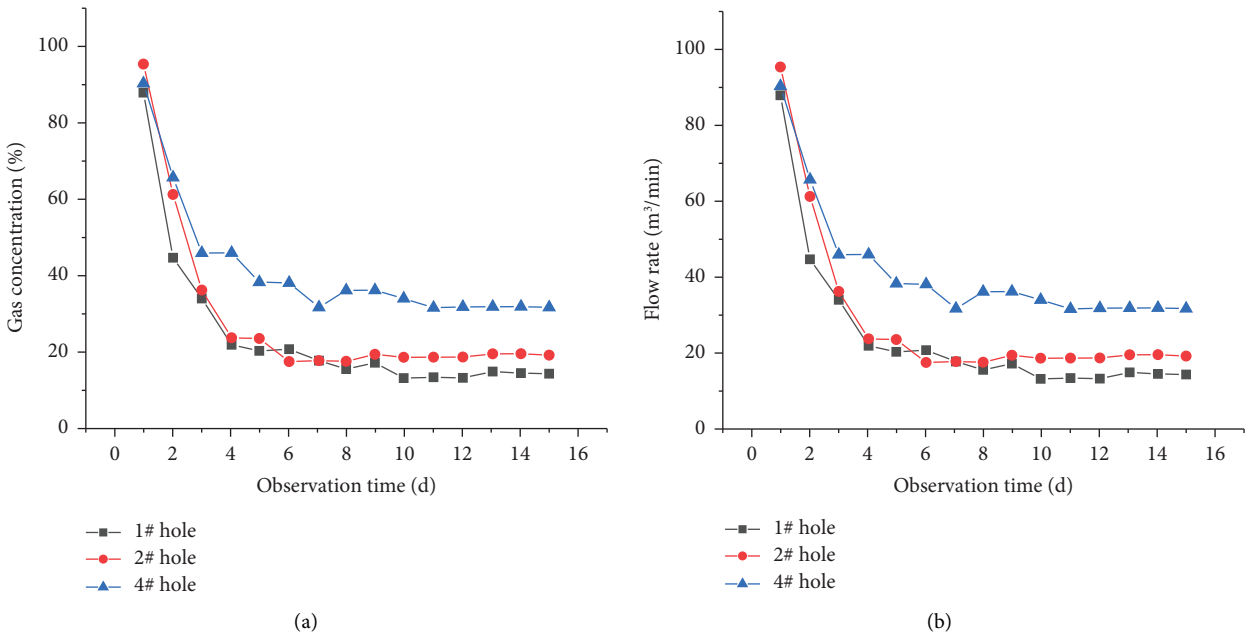

FIGURE 14: Change of gas extraction effect in each borehole. (a) Variation curve of gas concentration in each borehole. (b) Gas concentration change in each borehole.

investment encompasses hydraulic fracturing equipment and technology, as well as geological exploration. Operating costs involve material, personnel, and environmental monitoring expenses. Long-term benefits include increased capacity and safety assurance. Overall, the economic feasibility and cost-effectiveness of segmented hydraulic fracturing depend on various factors. The use of segmented hydraulic fracturing technology for gas permeation in mines is primarily aimed at reducing the occurrence of gas-related accidents during the coal seam recovery process.

(2) The scalability and adaptability of segmented hydraulic fracturing technology in other coal mines may face challenges related to geological variations and investment costs. However, it also presents potential opportunities. Challenges include differences in geological conditions and investment costs. Potential opportunities involve increasing capacity and recovery rates, improving coal seam permeability, enhancing gas release, reducing the risk of gas explosions, and addressing subsidence issues in some mining scenarios. With continuous technological advancement and accumulated experience, one can anticipate broader applications of this technology in the coal mining industry. When promoting its use, a balance must be sought between economic, environmental, and social sustainability to ensure the successful application of the technology.

(3) The potential impact of hydraulic fracturing technology on coal seam permeability and gas extraction efficiency depends on various factors, including operational parameters, geological conditions, and equipment technology. When applying hydraulic fracturing technology, a careful assessment and monitoring of its actual effects on coal seam productivity and gas extraction are essential to ensure the feasibility and sustainability of the technology.

6. Conclusion

(1) Staged hydraulic fracturing is set to augment traditional hydraulic fracturing techniques. Unlike conventional hydraulic fracturing where pressure is concentrated at a single point for fracture initiation, staged hydraulic fracturing involves a more focused action point. This approach reduces seepage water pressure, elevates effective water pressure, and allows for achieving a controlled and reduced flow. The focal point of action is comparatively concentrated. Effective fracture management minimizes water flow, leading to a significant reduction in hydraulic system fracturing requirements, a drastic decrease in equipment demands, and increased suitability for underground roadway conditions.

(2) A three-dimensional model, developed using ABAQUS numerical simulation software, is employed to simulate staged hydraulic fracturing. The coal and rock mass subjected to compression fractures exhibits an oval form in terms of stress, strain, and crack propagation width. The strain cloud diagram mirrors the stress cloud diagram inversely, indicating higher stress levels around the ellipse periphery and lower stress in the center. With the injection of water pressure, the crack propagation width initially expands before gradually contracting, with a diminishing amplitude of each change.

(3) Analysis of the extraction outcomes poststaged hydraulic fracturing reveals a 1.73-fold increase in the average gas extraction concentration during the observation period. The average mixed flow rate experiences a 2.16-fold increase, and the average gas extraction purity is enhanced by 3.10 times. Staged hydraulic fracturing proves effective in boosting gas extraction efficiency while simultaneously reducing the gas content in coal seams. Moreover, the utilization of straightforward and reusable equipment in hydraulic fracturing alleviates pressure on coal and rock strata, mitigates tension, and minimizes the risk of rock rupture. This approach holds promising economic advantages and diverse application possibilities. The research findings provide new means for safe and efficient coal mining, particularly in enhancing gas extraction efficiency, alleviating strata pressure, and preventing gas disasters.

Data Availability

The data used to support the findings of this study are available from the corresponding author upon request.

Conflicts of Interest

The authors declare that they have no conflicts of interest regarding the publication of this paper.

References

[1] H. Zhou, J. Gao, K. Han, and Y. Cheng, "Permeability enhancements of borehole outburst cavitation in outburst-prone coal seams," *International Journal of Rock Mechanics and Mining Sciences*, vol. 111, pp. 12–20, 2018.

[2] Y. Yu, J. Liu, Y. Yang, D. Wu, W. Zhai, and F. Miao, "Experimental study on coal seam permeability enhancement and CO2 permeability caused by supercritical CO2," *Frontiers in Earth Science*, vol. 10, pp. 1–9, 2023.

[3] J. Huang, G. Xu, Y. Chen, and Z. Chen, "Simulation of microwave's heating effect on coal seam permeability enhancement," *International Journal of Mining Science and Technology*, vol. 29, no. 5, pp. 785–789, 2019.

[4] G. Cheng, B. Deng, Y. Liu et al., "Experimental investigation on the feasibility and efficiency of shear-fracturing stimulation for enhancing coal seam permeability," *Journal of Natural Gas Science and Engineering*, vol. 81, Article ID 103381, 2020.

[5] Y. Lu, Z. Ge, F. Yang, B. Xia, and J. Tang, "Progress on the hydraulic measures for grid slotting and fracking to enhance coal seam permeability," *International Journal of Mining Science and Technology*, vol. 27, no. 5, pp. 867–871, 2017.

[6] A. He, H. Fu, B. Huo, and C. Fan, "Permeability enhancement of coal seam by lower protective layer mining for gas outburst prevention," *Shock and Vibration*, vol. 2020, Article ID 8878873, 12 pages, 2020.

[7] T. Wang, W. Hu, D. Elsworth et al., "The effect of natural fractures on hydraulic fracturing propagation in coal seams," *Journal of Petroleum Science and Engineering*, vol. 150, pp. 180–190, 2017.

[8] H. Zhao, X. Wang, Z. Liu, Y. Yan, and H. Yang, "Investigation on the hydraulic fracture propagation of multilayers-commingled fracturing in coal measures," *Journal of Petroleum Science and Engineering*, vol. 167, pp. 774–784, 2018.

[9] Y. Liu, D. Tang, H. Xu, S. Li, and S. Tao, "The impact of coal macrolithotype on hydraulic fracture initiation and propagation in coal seams," *Journal of Natural Gas Science and Engineering*, vol. 56, pp. 299–314, 2018.

[10] S. Lyu, S. Wang, X. Chen et al., "Natural fractures in soft coal seams and their effect on hydraulic fracture propagation: a field study," *Journal of Petroleum Science and Engineering*, vol. 192, Article ID 107255, 2020.

[11] Z. Ge, S. Li, Z. Zhou, Y. Lu, B. Xia, and J. Tang, "Modeling and experiment on permeability of coal with hydraulic fracturing by stimulated reservoir volume," *Rock Mechanics and Rock Engineering*, vol. 52, no. 8, pp. 2605–2615, 2019.

[12] D. Wang, P. Zhang, J. Wei, and C. Yu, "The seepage properties and permeability enhancement mechanism in coal under temperature shocks during unloading confining pressures," *Journal of Natural Gas Science and Engineering*, vol. 77, Article ID 103242, 2020.

[13] D. Wang, T. Xiaorui, J. Wei et al., "Fracture evolution and nonlinear seepage characteristic of gas-bearing coal using X-ray computed tomography and the lattice Boltzmann method," *Journal of Petroleum Science and Engineering*, vol. 211, Article ID 110144, 2022.

[14] Y. Xue, P. G. Ranjith, F. Gao, Z. Zhang, and S. Wang, "Experimental investigations on effects of gas pressure on mechanical behaviors and failure characteristic of coals," *Journal of Rock Mechanics and Geotechnical Engineering*, vol. 15, no. 2, pp. 412–428, 2023.

[15] Y. Konno, Y. Jin, J. Yoneda, T. Uchiumi, K. Shinjou, and J. Nagao, "Hydraulic fracturing in methane-hydrate-bearing sand," *RSC Advances*, vol. 6, no. 77, pp. 73148–73155, 2016.

[16] Q. Cheng, B. Huang, and X. Zhao, "Numerical investigation on the mechanism of rock directional fracturing method controlled by hydraulic fracturing in dense linear multiholes," *Shock and Vibration*, vol. 2020, Article ID 6624047, 10 pages, 2020.

[17] Z. Xiao and K. Hongpu, "Pressure relief mechanism of directional hydraulic fracturing for gob-side entry retaining and its application," *Shock and Vibration*, vol. 2021, Article ID 6690654, 8 pages, 2021.

[18] X. Liu, Z. Qu, T. Guo et al., "An innovative technology of directional propagation of hydraulic fracture guided by radial holes in fossil hydrogen energy development," *International Journal of Hydrogen Energy*, vol. 44, no. 11, pp. 5286–5302, 2019.

[19] J. Li, B. Jia, C. Zhang, and W. Wang, "Seepage mechanism technical practice of hydraulic fracturing of coal seam and auxiliary image simulation technology," *Journal of Visual Communication and Image Representation*, vol. 59, pp. 244–252, 2019.

[20] Y. Shang, G. Wu, Q. Liu, D. Kong, and Q. Li, "The drainage horizon determination of high directional long borehole and gas control effect analysis," *Advances in Civil Engineering*, vol. 2021, Article ID 3370170, 11 pages, 2021.

[21] D. Kong, Q. Li, G. Wu, and G. Song, "Characteristics and control technology of face-end roof leaks subjected to repeated mining in close-distance coal seams," *Bulletin of Engineering Geology and the Environment*, vol. 80, no. 11, pp. 8363–8383, 2021.

[22] Z.-X. Xie, X.-G. Wu, T.-D. Long et al., "Visualization of hydraulic fracture interacting with pre-existing fracture," *Petroleum Science*, vol. 20, no. 6, pp. 3723–3735, 2023.
[23] E. Detournay, "Slickwater hydraulic fracturing of shales," *Journal of Fluid Mechanics*, vol. 886, pp. F1–F6, 2020.
[24] T. Liu, Y. Sheng, Q. Li et al., "Hydraulic fracture propagation in fractured rock mass," *Applied Sciences*, vol. 12, p. 5846, 2022.
[25] Q. Ye, G. Wang, Z. Jia, C. Zheng, and W. Wang, "Similarity simulation of mining-crack-evolution characteristics of overburden strata in deep coal mining with large dip," *Journal of Petroleum Science and Engineering*, vol. 165, pp. 477–487, 2018.
[26] J. Wei, S. Huang, G. Hao, J. Li, X. Zhou, and T. Gong, "A multi-perforation staged fracturing experimental study on hydraulic fracture initiation and propagation," *Energy Exploration and Exploitation*, vol. 38, no. 6, pp. 2466–2484, 2020.
[27] H. Ma, J. Wang, J. Qian, and Q. Luo, "Mesoscopic deformation of a hydraulic and mechanical aperture of a single fracture under normal stress," *Lithosphere*, vol. 2023, pp. 1–12, 2023.
[28] D. Xiong and X. Ma, "Influence of natural fractures on hydraulic fracture propagation behaviour," *Engineering Fracture Mechanics*, vol. 276, Article ID 108932, 2022.
[29] Q. Li, G. Wu, D. Kong, S. Han, and Z. Ma, "Study on mechanism of end face roof leaks based on stope roof structure movement under repeated mining," *Engineering Failure Analysis*, vol. 135, Article ID 106162, 2022.
[30] Y. Liu, X. Zheng, X. Peng, Y. Zhang, H. Chen, and J. He, "Influence of natural fractures on propagation of hydraulic fractures in tight reservoirs during hydraulic fracturing," *Marine and Petroleum Geology*, vol. 138, Article ID 105505, 2022.
[31] G. Yang, W. Hu, S. Tang, Z. Zhou, and Z. Song, "Impacts of vertical variation of coal seam structure on hydraulic fracturing and resultant gas and water production: a case study on the shizhuangnan block, southern qinshui basin, China," *Energy Exploration and Exploitation*, vol. 42, no. 1, pp. 52–64, 2023.
[32] L. C. Wang, Y. Xue, Z. Z. Cao, H. L. Kong, J. Y. Han, and Z. Z. Zhang, "Experimental study on mode I fracture characteristics of granite after low temperature cooling with liquid nitrogen," *Water*, vol. 15, no. 19, p. 3442, 2023.
[33] Y. Shang, L. Zhang, D. Kong, Y. Wang, and Z. Cheng, "Overlying strata failure mechanism and gas migration law in close distance outburst coal seams: a case study," *Engineering Failure Analysis*, vol. 148, Article ID 107214, 2023.
[34] X. Men, J. Li, and Z. Han, "Fracture propagation behavior of jointed rocks in hydraulic fracturing," *Advances in Materials Science and Engineering*, vol. 2018, Article ID 9461284, 12 pages, 2018.
[35] S. Wang, H. Li, and D. Li, "Numerical simulation of hydraulic fracture propagation in coal seams with discontinuous natural fracture networks," *Processes*, vol. 6, no. 8, p. 113, 2018.
[36] C. Sun, H. Zheng, W. D. Liu, and W. Lu, "Numerical simulation analysis of vertical propagation of hydraulic fracture in bedding plane," *Engineering Fracture Mechanics*, vol. 232, Article ID 107056, 2020.
[37] X. Liu, Y. Sun, T. Guo, M. Rabiei, Z. Qu, and J. Hou, "Numerical simulations of hydraulic fracturing in methane hydrate reservoirs based on the coupled thermo-hydrologic-mechanical-damage (THMD) model," *Energy*, vol. 238, Article ID 122054, 2022.
[38] W. Lu and C. He, "Numerical simulation of the laws of fracture propagation of multi-hole linear Co-directional hydraulic fracturing," *Energy Exploration and Exploitation*, vol. 39, no. 3, pp. 903–926, 2021.
[39] T. Guo, Z. Qu, D. Gong, X. Lei, and M. Liu, "Numerical simulation of directional propagation of hydraulic fracture guided by vertical multi-radial boreholes," *Journal of Natural Gas Science and Engineering*, vol. 35, pp. 175–188, 2016.
[40] X. Li, X. Qu, T. Sun et al., "Numerical simulation of hydraulic fracturing effect based on abaqus," *IOP Conference Series: Materials Science and Engineering*, vol. 744, no. 1, pp. 012010–012015, 2020.